

RSC Advances



This is an *Accepted Manuscript*, which has been through the Royal Society of Chemistry peer review process and has been accepted for publication.

Accepted Manuscripts are published online shortly after acceptance, before technical editing, formatting and proof reading. Using this free service, authors can make their results available to the community, in citable form, before we publish the edited article. This *Accepted Manuscript* will be replaced by the edited, formatted and paginated article as soon as this is available.

You can find more information about *Accepted Manuscripts* in the [Information for Authors](#).

Please note that technical editing may introduce minor changes to the text and/or graphics, which may alter content. The journal's standard [Terms & Conditions](#) and the [Ethical guidelines](#) still apply. In no event shall the Royal Society of Chemistry be held responsible for any errors or omissions in this *Accepted Manuscript* or any consequences arising from the use of any information it contains.

Unusual solvent-mediated hydrolysis of dicarboxylate monoester ligands in copper(II) complexes toward simultaneous crystallization of new dicarboxylate derivatives

Jayanta Kumar Nath,[†] Alexander M. Kirillov[‡] and Jubaraj B. Baruah*[†]

[†]Department of Chemistry, Indian Institute of Technology Guwahati, Guwahati 781 039 Assam, India,
Fax: + 91-361-2690762; Ph. + 91-361-2582311;
email: juba@iitg.ernet.in; Url: <http://www.iitg.ac.in/juba>

[‡]Centro de Química Estrutural, Complexo I, Instituto Superior Técnico, Universidade de Lisboa, Av. Rovisco Pais, 1049-001, Lisbon, Portugal.

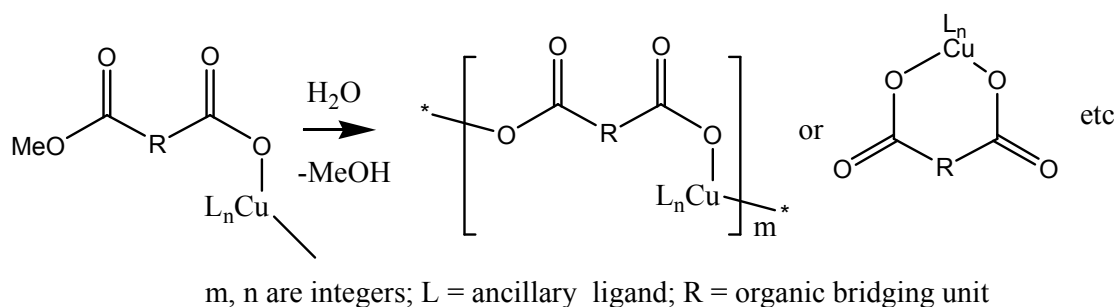
Abstract:

A series of copper(II) complexes [Cu(cmb)₂(im)₂] (**1**), [Cu(cmn)₂(im)₄] (**3**) and [Cu(cmp)₂(im)₂] (**5**) bearing various dicarboxylate monoester derivatives [cmb = 2-carbomethoxy-benzoate; cmn = 8-carbomethoxy-naphthalene-1-carboxylate; cmp = 2-carbomethoxy-phenyl-2-benzoate] were generated from copper(II) acetate, imidazole (im) and an aromatic anhydride [phthalic, 1,8-naphthalic or biphenic anhydride for **1**, **3** or **5**, respectively]. Unusual solvent-mediated transformations of the crystals of two copper dicarboxylate monoester complexes to new crystals of corresponding dicarboxylate derivatives by hydrolysis of ester groups were observed and investigated in detail. Thus, crystals of **1** underwent transformation to the crystals of copper(II) phthalate 2D coordination polymer {[Cu₂(pht)₂(im)₄·H₂O]·H₂O}_n (**2**) (pht = phthalate) on moistening with aqueous methanol. Similarly, the crystals of **3** after wetting with aqueous dimethylformamide (DMF) were transformed to the crystals of a metallacycle [Cu(nap)(im)(DMF)(H₂O)]₂ (**4**) (nap = 1,8-naphthalenedicarboxylate). In contrast to **1** and **3**, the crystals of **5** were found to be stable under ambient conditions. The compounds **1–5** have been characterized by IR and UV-vis spectroscopy, single crystal and powder X-ray diffraction methods. Topological analysis showed that in the **1**→**2** transformation an overall 2D network topology was modified from the 4-connected H-bonded **sql** net [Shubnikov tetragonal plane net] to 3-connected metal-organic **hcb** net [Shubnikov hexagonal plane net/(6,3)], whereas no topology change was detected during an analogous **3**→**4** transformation, with both structures exhibiting the topologically equal H-bonded **sql** nets.

Introduction:

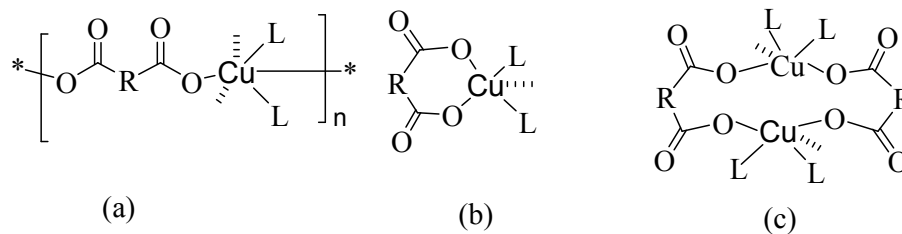
Isolation and characterization of intermediate metal complexes formed during hydrolysis of esters provide understanding on active sites of metallohydrolases.¹ Copper complexes are widely used in the hydrolysis reactions of esters,² anhydrides,³ lactones⁴ and imides.⁵ Enantioselective hydrolysis of α -amino acid esters is catalyzed by copper complexes⁶ and thus there is a challenge to make model intermediate Cu

derivatives.⁷ Copper(II) ions cause methanolysis of amides⁸ in which tetrahedral copper(II) complexes serve as intermediate species.⁹ In copper complexes catalyzed ester hydrolysis, coordination of copper ion facilitates intramolecular nucleophilic attack on the C=O group and subsequently it assists departure of leaving group.¹⁰ Catalytic hydrolysis of phosphate esters by copper ions find use in DNA cleavage reactions,¹¹ phosphodiesterases^{1c} and in artificial nucleases.¹² There are also examples of Cu-catalyzed hydrolysis operating simultaneously with molecular recognition.¹³ Copper containing metallosurfactants are useful in ester hydrolysis,¹⁴ while some copper complexes can hydrolyze polyester-based hydrogels.¹⁵ It is clear from the foregoing discussion that the type of hydrolysis shown in equation 1 can be of significant importance toward understanding related biotransformations and designing alternative hydrolysis methods useful in coordination and materials chemistry. For example, study of such reactions in solvent-free conditions can lead to novel green reaction protocols and their implications will be close to biological process which itself does not use solvent in the way a reaction carried out in solution. Advantage of these reactions without a solvent or with a minimal amount of solvent would allow the replacement of a methyl ester group by water molecule, thus causing minimum size variation in the structure while the methanol byproduct will easily diffuse or evaporate.



Equation 1: Hydrolysis of dicarboxylate monoester copper(II) complex.

It is expected that hydrolysis in confined medium would help to adopt selectively any of the possible binding modes depicted in Figure 1. Since there are examples on hydrolysis of metal complexes having lipophilic imidazole ligands,¹⁶ we have chosen imidazole as the ancillary ligand to examine model reactions for hydrolysis in solid state. Hence, we report here the unusual hydrolysis of crystals of dicarboxylate monoester copper(II) complexes which, upon moistening with a minimum amount of solvent, are directly transformed into new crystals of dicarboxylate derivatives, as well as discuss the structural and topological relationship between the reactants and products.

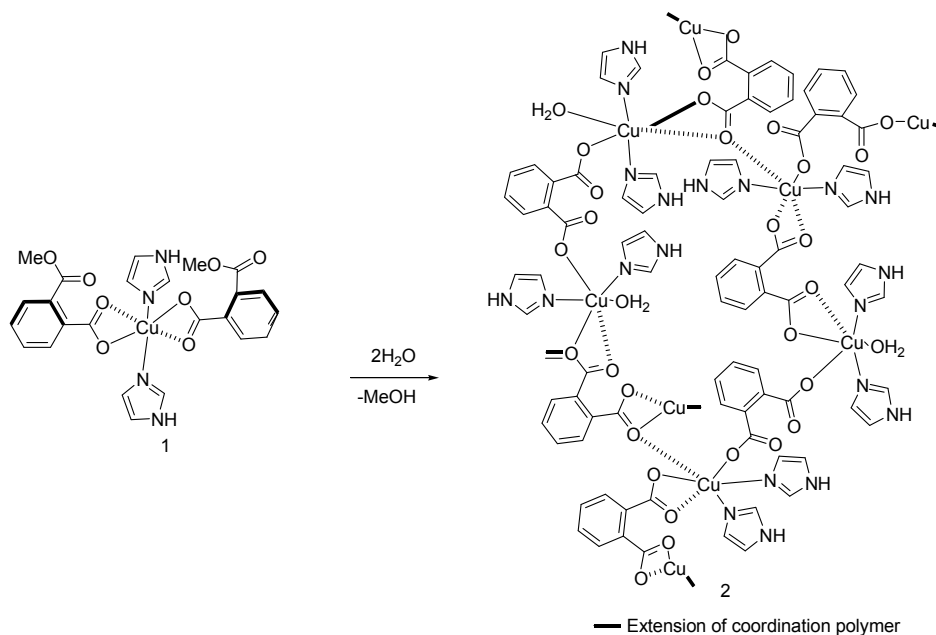


Where L = ancillary ligand, R is aliphatic or aromatic bridging unit, n is an integer

Figure 1: Some representative ways of dicarboxylate binding by copper(II) ions.

Results and discussion:

The crystals of a mononuclear complex di-imidazole di-(2-carbomethoxy-benzoato)copper(II), $[\text{Cu}(\text{cmb})_2(\text{im})_2]$ (where cmb = 2-carbomethoxy-benzoate; im = imidazole) (**1**), could be easily obtained from the reaction of phthalic anhydride with copper(II) acetate in methanol. Crystals of **1** which has visible absorption at 651 nm (supporting figure 1S) are unstable in humid environment or when contacting with aqueous methanol. These crystals, without getting fully dissolved in methanol, transformed to new crystals of a copper(II) phthalate coordination polymer $\{[\text{Cu}_2(\text{pht})_2(\text{im})_4 \cdot \text{H}_2\text{O}] \cdot \text{H}_2\text{O}\}_n$ (pht = phthalate anion, im = imidazole) (**2**). Reaction involved in this transformation is shown in Scheme 1. Crystals of **2** have a visible absorption at 723 nm and are generally smaller in size compared to those of **1**. Morphologies of crystals of complex **1** and dicarboxylate coordination polymer **2** are well distinguishable, which are shown as supporting Figures 2S.



Scheme 1: Transformation of complex **1** to coordination polymer **2**.

Initially we found the transformation of the crystals by observing the changes at the crystal morphology by naked eyes. This was further confirmed by microscopic views monitored as a lapse of time of a crystal

moistened with a minimum amount of methanol. The figure 2a shows microscopic view of morphology of a crystal of complex **1** placed on a glass plate at the beginning of observation. Figures 2b and 2c are photographs of particular crystal moistened with a minimum amount of methanol, which were recorded after every one hour time interval. From these figures it is evident that parent crystal got transformed to another form of crystals through parturition of light blue crystals on the side and surface of the parent crystal. The blue crystals felt apart and they could be separated easily and characterized. We have determined the single crystal X-ray structure of the crystals obtained and confirmed them to be coordination polymer **2**. We have checked powder XRD-pattern and also IR spectra of such crystals obtained during bulk conversion and confirmed bulk transformation of crystals of complex **1** to crystals of coordination polymer **2**.

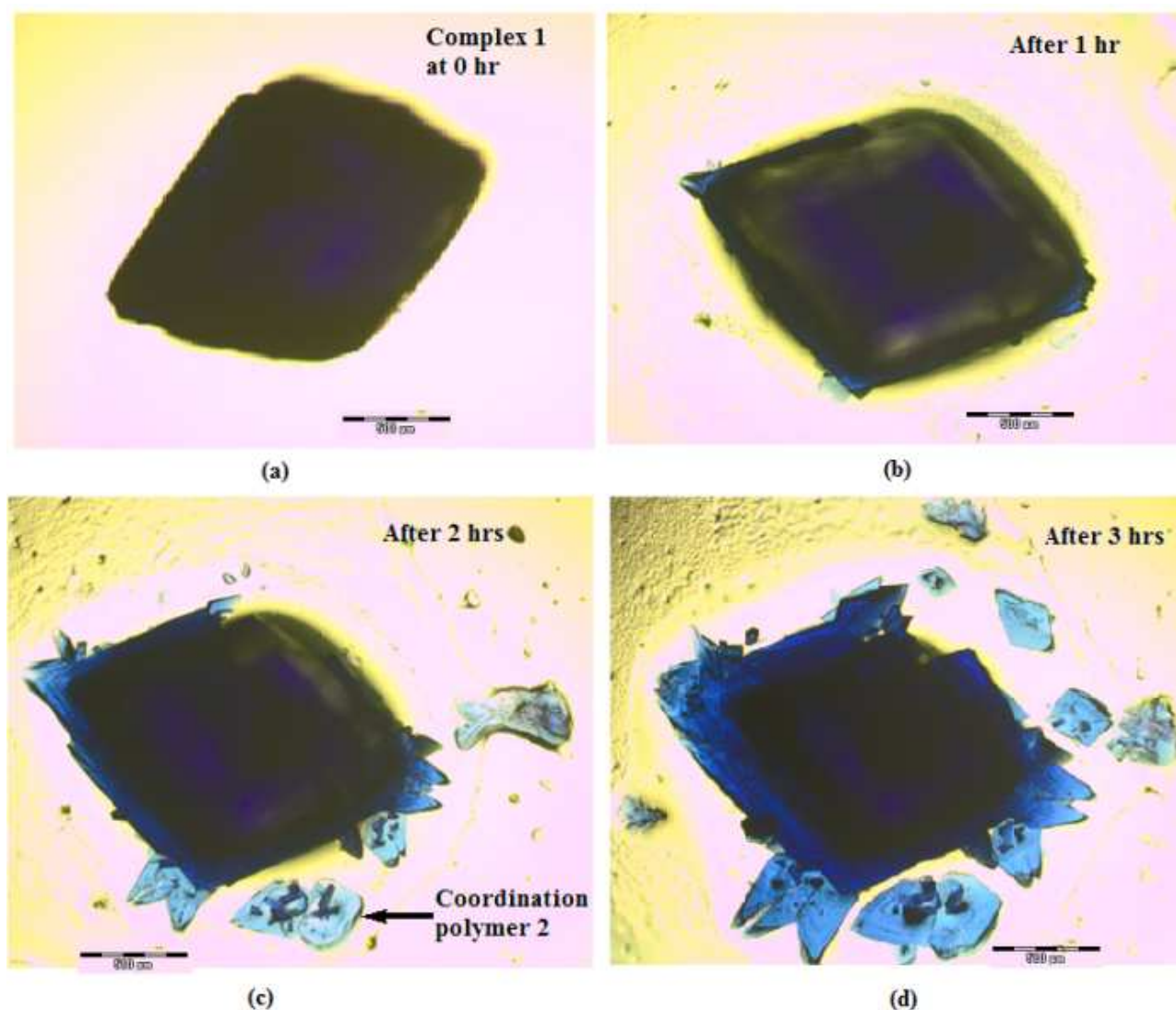
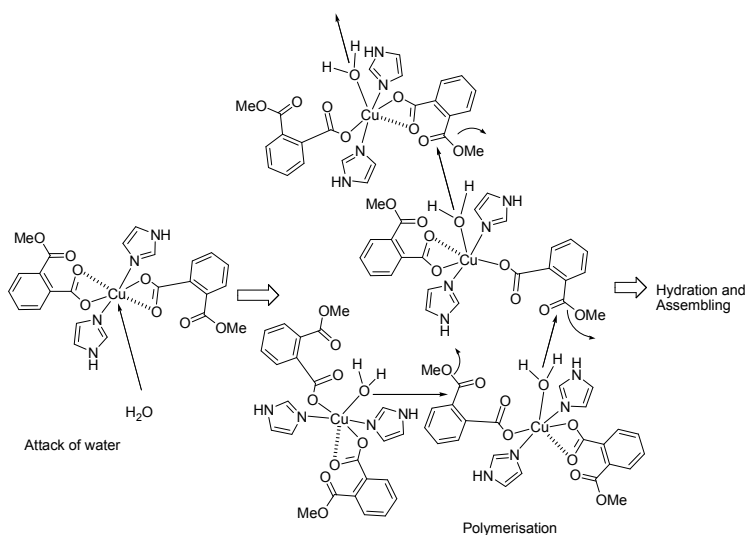


Figure 2: (a) Photograph of a crystal of complex **1**. (b–d) Photograph of partially transformed crystal of the complex **1** wetted by methanol under ambient conditions after (b) 1 h, (c) 2 h and (d) 3 h.

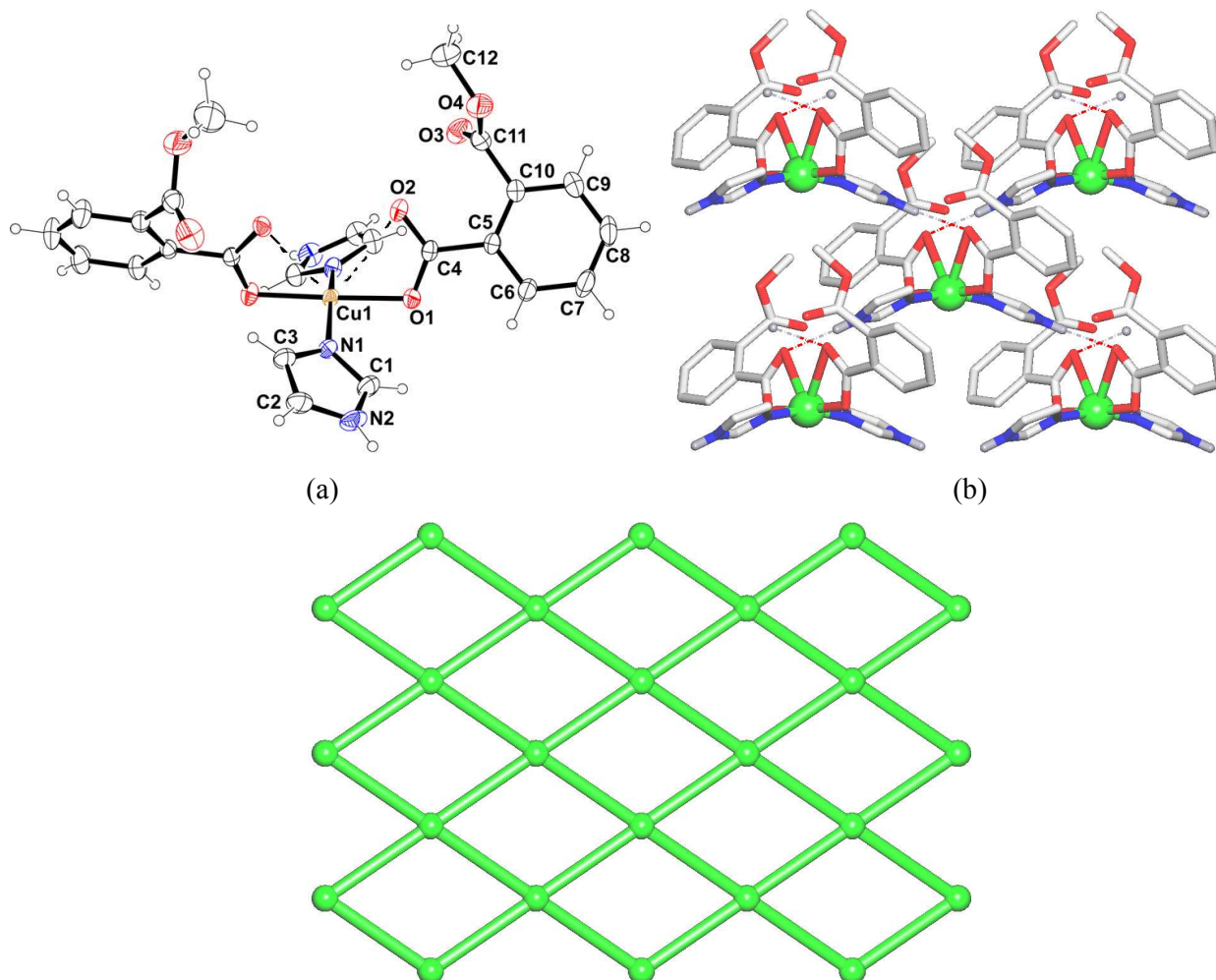
These observations clearly show that during hydrolysis one form of crystal gradually transforms to another form of crystal. A proposed mechanism of such transformation is shown in Scheme 2. The ester functional group present in the complex **1** has a strong stretching vibration at 1730 cm^{-1} (supporting figure 3S). This band is absent in the IR spectrum of the crystals of coordination polymer **2**. For comparison, the overlaid IR spectra of the bulk samples before and after the transformation are shown in supporting Figure 3S. The solid state UV-visible absorbance spectra of the complex **1** and the coordination polymer **2** are clearly distinguishable, with an adsorption at 651 nm or 723 nm corresponding to the d-d transition of the d^9 -copper(II) ion in **1** or **2**, respectively. The ESI-MS(+) spectrum of compound **1** in MeOH shows a characteristic signal at $m/z = 423$, which indicates an easy dissociation of two imidazole ligands in solution leading to $[\text{Cu}(\text{cmb})_2 + \text{H}]^+$ species. This fact also explains a low yield of **2** in solution synthesis, while the solid phase transformation of **1** to **2** is quantitative.



Scheme 2: A proposed mechanism for hydrolysis of **1**.

Although model intermediate tetrahedral copper complexes have been earlier reported for methanolysis reactions,^{8,9} we find that **1** is a six-coordinated compound having two weak coordination bonds. Crystal structure of **1** is highly symmetric (Figure 3a) and copper ion lies on a twofold axis and only half of the molecule was observed in its asymmetric unit. It contains a copper(II) ion that is coordinated to one 2-carbomethoxybenzoate and an imidazole ligand. The complex **1** has a copper(II) ion with a distorted octahedral geometry (Figure 3a), filled by two bis-chelating carboxylate ligands and two imidazole moieties. Cu1-O1 and Cu-N1 bond distances of 1.9637(14) and 1.9788(17) Å, respectively, support that these are strong dative bonds. On the other hand, the Cu1-O2 distance of 2.74 Å is indicative of rather weak interaction of O2 with the copper ion. It may be suggested that the steric congestion arising from the

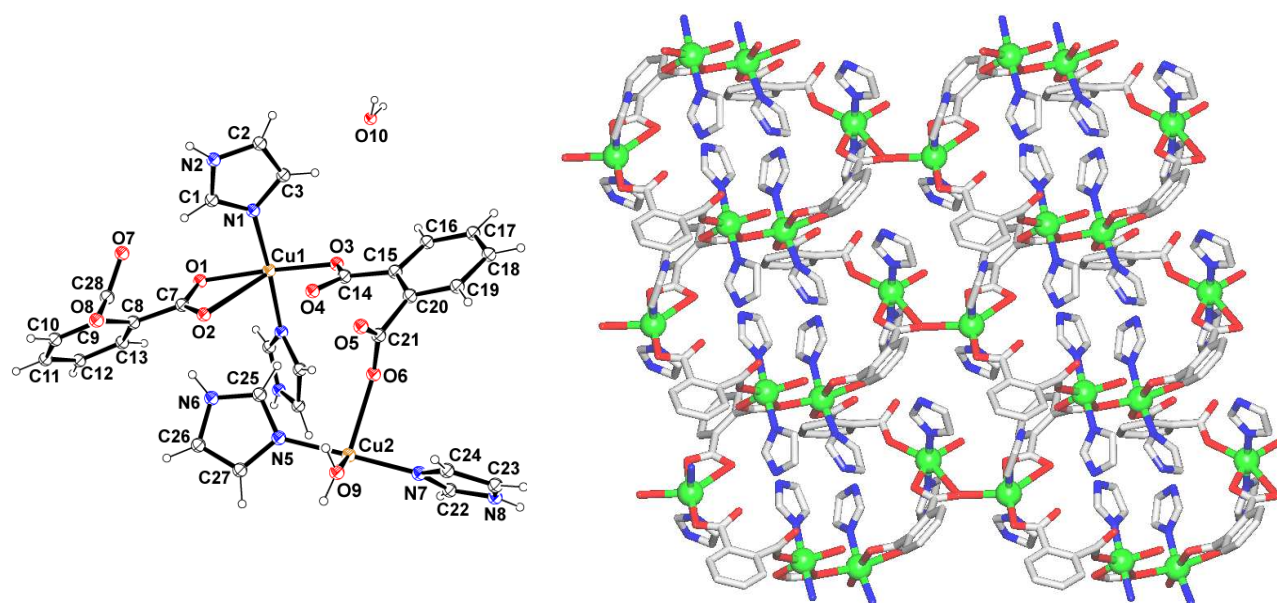
presence of the carbomethoxy groups twists the carboxylate ligands to reduce their chelation ability. It is interesting to note that the $\angle\text{N1-Cu1-N1}$ bond angle of $164.63(11)^\circ$ deviates by about 15° from 180° to have its contribution to adopt an octahedral geometry, thus showing that the two imidazole moieties are not exactly at mutual *trans* positions. Due to the positioning of these ligands in such a manner, the copper ion is slightly exposed from one direction for approach of an external ligand. Such geometry provides more open space on one side of the distorted octahedron and helps an approaching of water molecules to coordinate to copper ion, thus facilitating the hydrolysis of the ester groups. The steric factor of the carbomethoxy group influences the structure as despite of having long Cu-O2 bond distances, we did not observe the commonly formed dimeric paddle-wheel structures in related copper carboxylate complexes. Besides, the discrete monocopper(II) $[\text{Cu}(\text{cmb})_2(\text{im})_2]$ blocks in the structure of **1** are assembled, via the repeating $\text{N2-H2A}\cdots\text{O2}$ hydrogen bonds, into a 2D H-bonded network (Figure 3b). It has been analyzed from the topological viewpoint following the concept of the simplified underlying net.^{17a-d} After contracting the molecular $[\text{Cu}(\text{cmb})_2(\text{im})_2]$ units to the respective centroids, an underlying network has been obtained (Figure 3c). It is topologically described as a uninodal 4-connected net with the **sql** [Shubnikov tetragonal plane net] topology and the point symbol of $(4^4\cdot6^2)$.^{17a,17e}



(c)

Figure 3: Structural fragments of complex **1**. (a) Ellipsoid plot (50% probability). (b) H-bonding pattern showing interlinkage of monocopper(II) units into a 2D H-bonded layer; H atoms apart from those of H-bonds are omitted for clarity; color codes: Cu green balls, O red, N blue, C gray, H dark gray. (c) Topological representation of the simplified uninodal 4-connected 2D net with the **sql** topology and the point symbol of $(4^4 \cdot 6^2)$; green balls are the centroids of 4-connected $[\text{Cu}(\text{cmb})_2(\text{im})_2]$ nodes.

Asymmetric unit and the 2D metal-organic network of coordination polymer **2** are shown in Figures 4a and 4b, respectively. The 2D corrugated layer can be visualized as assemblies of $[\text{Cu}_5(\text{pht})_5]$ cyclic motifs driven by μ_2 - and μ_3 -phthalate moieties. The structure bears two different hexa-coordinate copper ions, of which Cu1 is coordinated by two imidazole ligands and three independent phthalate moieties (two μ_3 -pht and one μ_2 -pht) with the carboxylate groups adopting monodentate $\eta^1:\eta^0$ and bidentate $\eta^1:\eta^1$ and $\mu_2-\eta^2:\eta^1$ coordination modes. Other Cu2 ion is coordinated to a water molecule and two imidazole ligands, as well as to two independent μ_2 - and μ_3 -bridging phthalate dianions. Their carboxylate groups that are connected to the Cu2 atom exhibit the $\eta^1:\eta^0$ and $\mu_2-\eta^2:\eta^1$ coordination modes. Thus, by virtue of monodentate, bidentate and bifurcated coordination of the phthalate dianions, they act as linkers to copper ions in the 2D coordination polymer **2**. The Cu-N bond lengths vary between 1.965(3) and 1.981(3) Å, whereas the Cu-O bond distances are within the 2.007(3)-2.073(3) Å range, except the Cu2-O6 [2.309(3) Å], Cu1-O8 [2.499(3) Å] and Cu2-O8 [2.739(3) Å] bonds. The relatively higher bond length of the two later bonds is due to side on ($\mu-\eta^2$ -O type) bridging mode with copper(II). These distances are within the admissible range reported for similar coordination modes in other copper complexes^{18a} and are also below the sum of the van der Waals radii of the Cu and O atoms [2.92 Å].^{18b}



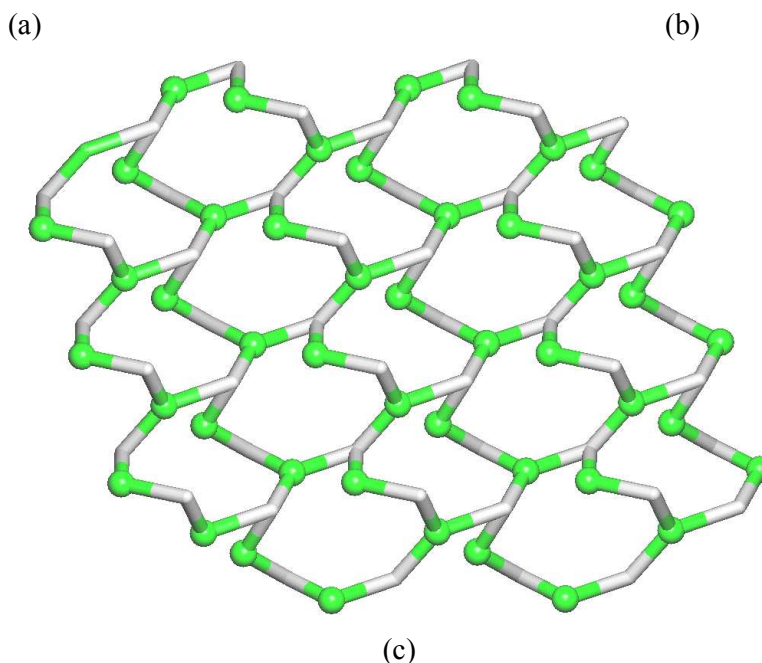


Figure 4: Structural fragments of the coordination polymer **2**. (a) Ellipsoid plot (50% probability) of the asymmetric unit. (b) 2D metal-organic layer; H atoms and solvent molecules are omitted for clarity; color codes: Cu green balls, O red, N blue, C gray. (c) Topological representation of the simplified uninodal 3-connected 2D net with the **hcb** topology and the point symbol of (6^3) ; color codes: 3-connected Cu1 nodes and 2-connected Cu2 linkers (green balls), centroids of 3-connected μ_3 -pht nodes and 2-connected μ_2 -pht linkers (gray).

To better understand the 2D metal-organic network of **2**, we have also carried out its topological analysis by applying the above-mentioned concept of underlying net.^{17a-c} Such a net has been generated by reducing the phthalate blocks to their centroids and eliminating the terminal H₂O and imidazole ligands (Figure 4c). This net is thus composed of the topologically equivalent 3-connected Cu1 and μ_3 -pht nodes, as well as 2-connected Cu2 and μ_2 -pht linkers. Its topological analysis reveals a uninodal 3-connected network with the point symbol of (6^3) and **hcb** [Shubnikov hexagonal plane net/ $(6,3)$] topology, which is different from the **sql** net encountered in the compound **1**.

In **2**, both the crystallization and coordinated water molecules are anchored to the O atoms of the phthalate ligands through different O–H \cdots O hydrogen bonds, whereas N–H \cdots O interactions between the imidazole moieties and COO or H₂O groups provide further stabilization of the structure. As a result, these multiple intermolecular H-bonding interactions are responsible for the extension of 2D metal-organic layers to a very complex 3D supramolecular architecture. After simplification,^{17a} its topological analysis disclosed an intricate hexanodal 3,4,5,5,5,6-connected net with the unique topology described by the point symbol of $(4.5.6)(4^2.5^2.6.7)(4^3.5^2.6^4.7)(4^3.5^4.6.7.8)(4^5.5^2.6^3)(4^6.5^2.6^4.7^2.8)$.

The powder-XRD patterns of **1** and **2** were recorded and compared with the simulated ones generated from the single crystal X-ray diffraction data, indicating a rational correlation between them (Figure 5).

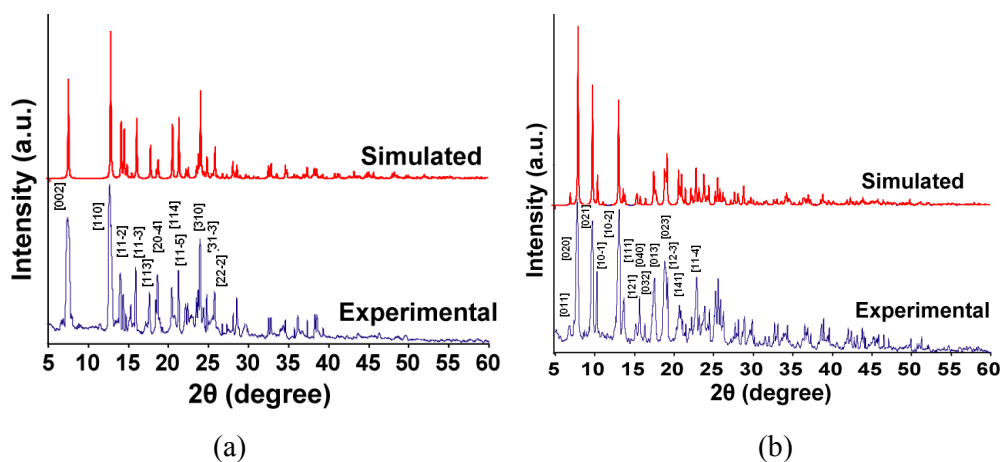
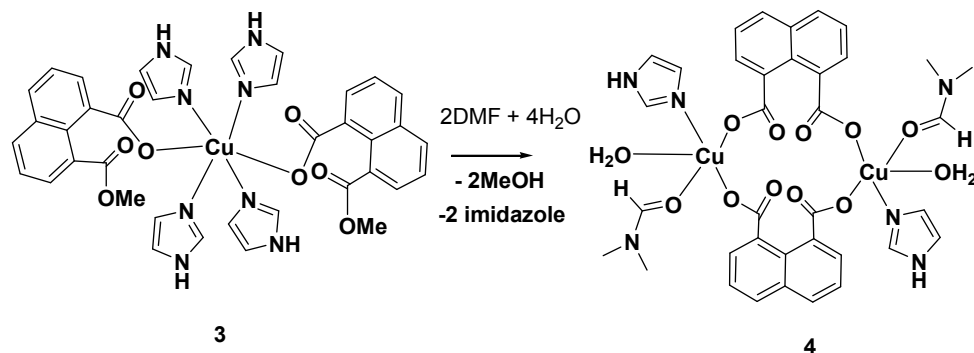


Figure 5: Powder-XRD patterns of the (a) complex **1** and (b) the coordination polymer **2**.

Crystals of complex **1** belong to $C2/c$ space group and have a unit cell volume of $2568.0(3) \text{ \AA}^3$, whereas the crystals of the coordination polymer **2** crystallize within $P2_1/n$ space group with a unit cell volume of $3101.33(19) \text{ \AA}^3$. A helical 1D copper(II) phthalate-imidazole coordination polymer¹⁹ was earlier prepared from the reaction of copper(II) carbonate with phthalic acid. Comparison of its structure with that of **2** (Scheme 1, Figure 4) has shown some differences in the coordination modes of phthalate moieties. In the 1D polymer,¹⁹ two copper(II) ions are interconnected via the $\eta^1:\eta^0$ and $\eta^1:\eta^1$ carboxylate groups of μ_2 -phthalate dianions, resulting in a helical 1D chain. Thus, the structure of the polymer formed through reaction in solution differs from the one that was generated via the solid state transformation of **1**.

We also studied reaction of copper(II) acetate with 1,8-naphthalic anhydride in presence of imidazole in methanol, which resulted in a mononuclear tetra-imidazole di-(8-carbomethoxy-naphthalene-1-carboxylato)copper(II) complex, $[\text{Cu}(\text{cmn})_2(\text{im})_4]$ (where $\text{cmn} = 8\text{-carbomethoxy-naphthalene-1-carboxylate}$) (**3**). The compound **3** is relatively unstable in comparison to the complex **1**. Although crystals of **3** have been of poor quality, we could determine the skeleton of the complex from the single crystal X-ray analysis. The complex has four coordinated nitrogen atoms of imidazole ligands in one plane around the copper(II) ion, while two monodentate 8-carbomethoxy-naphthalene-1-carboxylate ligands are in axial positions, thus forming the distorted octahedral geometry around the Cu(II) center (Figure 6a). The molecule of complex **3** has its Cu1 atom on an inversion centre the asymmetric unit is constituted by one 8-carbomethoxy-naphthalene-1-carboxylate anion and an imidazole molecule coordinated to copper ion. The observed lengths of the Cu1-N1, Cu1-N3 and Cu1-O2 bonds are $2.006(10)$, $2.014(12)$ and $2.468(8) \text{ \AA}$, respectively. The bulk purity of **3** has been confirmed by the experimental and simulated powder-XRD patterns (Figure 7) that show rather good matching. In **3**, the

discrete monocopper(II) $[\text{Cu}(\text{cmn})_2(\text{im})_4]$ units are held together through the intermolecular $\text{N2-H2A}\cdots\text{O1}$ and $\text{N4-H4A}\cdots\text{O1}$ hydrogen bonds, generating a 2D H-bonded network (Figure 6c). Interestingly, its topological analysis revealed a uninodal 4-connected **sql** net that is topologically similar to the H-bonded network of **1**.



Scheme 2: Transformation of complex 4 to dicopper(II) derivative 3.

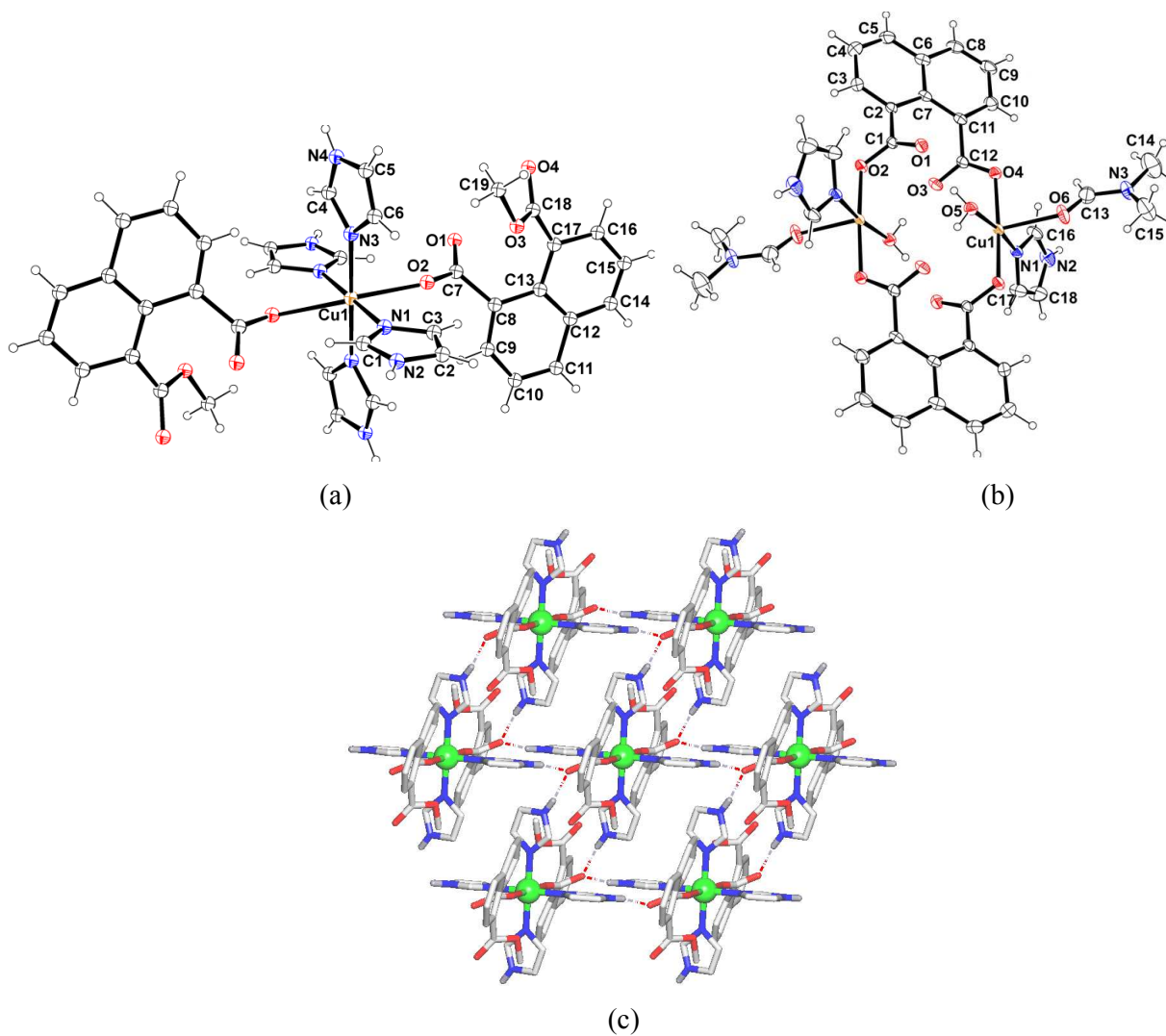
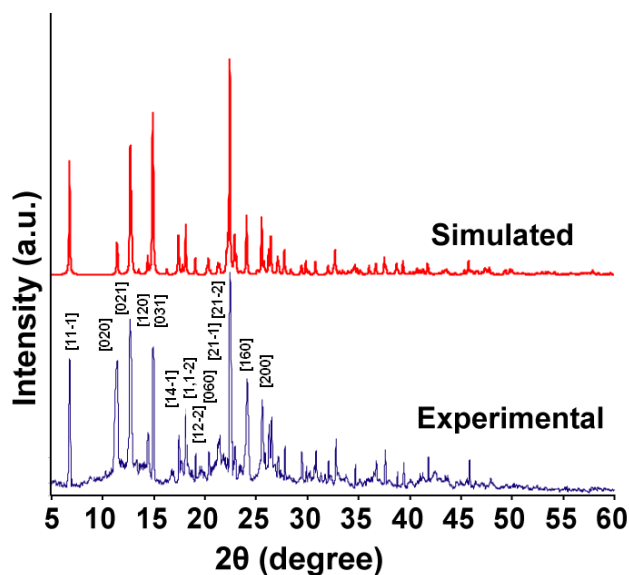


Figure 6: Ellipsoid plots (50% probability) of complexes **3** (a) and **4** (b). (c) H-bonding pattern of **3** showing the interlinkage of monocopper(II) units into a 2D H-bonded layer; H atoms apart from those of H-bonds are omitted for clarity; color codes: Cu green balls, O red, N blue, C gray, H dark gray.

It was earlier shown that the hydrolysis of 1,8-naphthalic anhydride in the presence of various metal ions resulted in metallacycles with different nuclearities.^{3c} In particular, an imidazole containing 1,4-naphthalene dicarboxylate copper(II) derivative was found to be a five-coordinate 1D coordination polymer.²⁰ Solid state or solvent-mediated reactions of 1,8-naphthalic anhydride to form imides,²¹ and reaction of co-crystals were reported earlier.²² In this study, we visually observed that the crystals of **3** which when moistened with aqueous dimethylformamide (DMF) undergo hydrolysis with simultaneous crystallization of new dinuclear metallacycle $[\text{Cu}(\text{nap})(\text{im})(\text{DMF})(\text{H}_2\text{O})]_2$ (**4**) (where nap = 1,8-naphthalene-dicarboxylate). The structure of the metallacycle **4** (Figure 6b) has two copper(II) ions in identical environment, which are interconnected by two independent μ_2 -1,8-naphthalene-dicarboxylate blocks wherein both COO groups acting in a $\eta^1:\eta^0$ -mode. Apart from two carboxylate oxygen atoms, the square-pyramidal environment of each copper ion is filled by H_2O , DMF and imidazole ligands. The dimeric complex lies about an inversion centre. The uncoordinated O atoms of COO groups of the 1,8-naphthalene-dicarboxylate ligands, as well as the water molecules on the two copper ions of the metallacycle are related by a center of inversion (Figure 6b). Thus, the transformation of the crystals of **3** on moistening with aqueous DMF resulted in the formation of the crystals of metallacycle **4**. Such transformation occurred as a consequence of ease in hydrolysis of ester group in the copper complex **3** to form a dicarboxylate derivative. This conversion was observed through naked eyes, as the blue colored crystals turned green once the crystals of **3** were suspended in aqueous DMF (supporting Figure 7S).



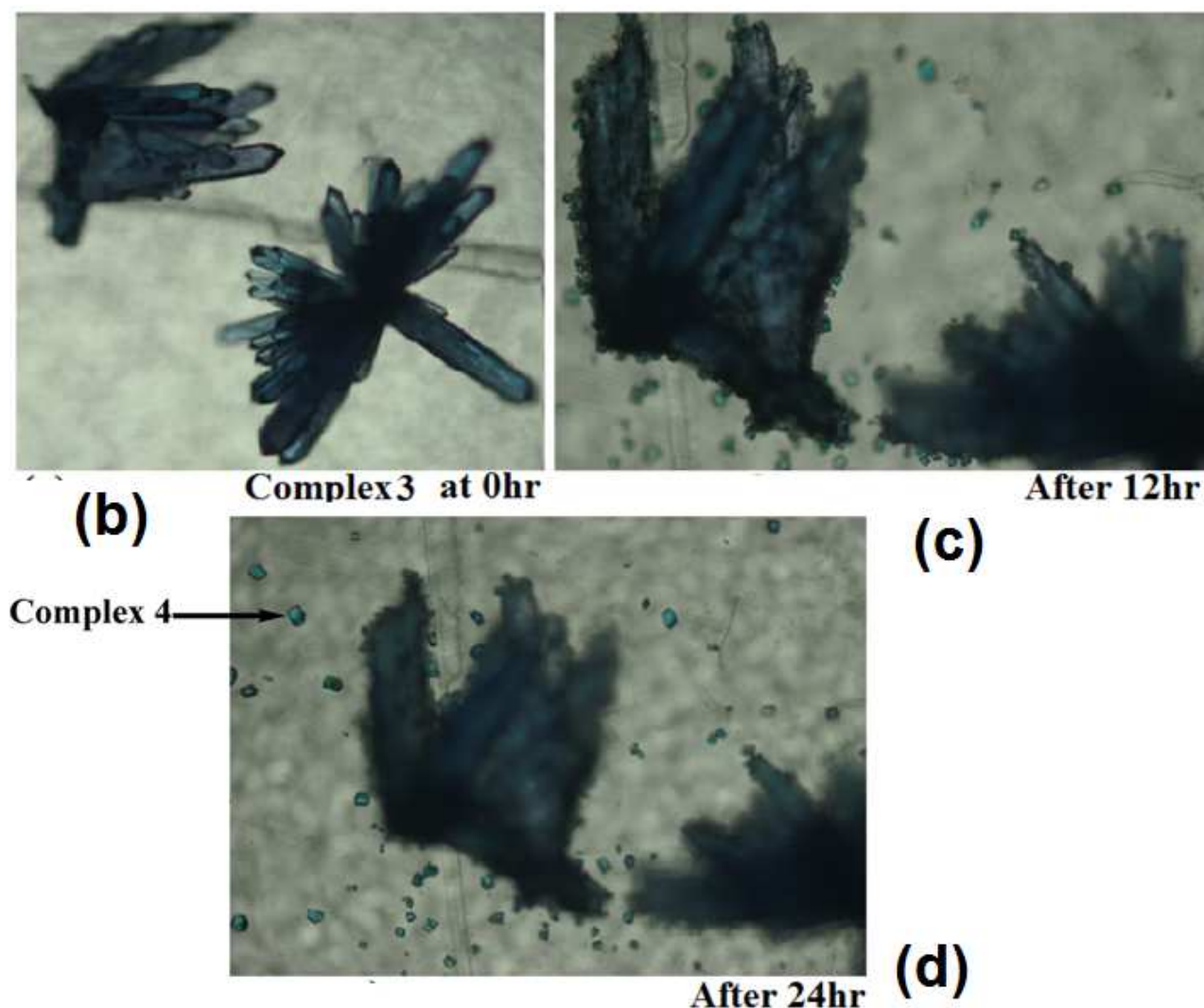


Figure 7: (a) Experimental and simulated powder-XRD patterns of complex **3**. (b) Transformation of complex **3** to complex **4** (b) at initial time (c) after 12 hrs, (d) after 24 hrs.

In solid state complex **3** has visible absorption at 553 nm, whereas metallacycle **4** absorbs at 711 nm, arising from d-d transition of d^9 -copper ions. Complex **3** has IR stretching at 1740 cm^{-1} due to ester functional group, while this band is absent in **4** (supporting figure 5S). Although in contrast to monocopper(II) units of **3**, the discrete structure of **4** is composed of dicopper(II) blocks, these are also arranged by intermolecular H-bonds into a 2D hydrogen bonded network, the topological analysis of which reveals the same **sql** topology as in **3**. Changes of the crystals of complex **3** was monitored with time and found that complex **4** was formed as the wet sample of **3** was left under ambient condition. Finally crystals of complex **4** was formed (figure 7b-d). Hence, conversion of **3** to **4** does not lead to the network topology change which, however, is observed during the transformation of **1** to **2**. Powder XRD pattern of metallacycle **4** was recorded and compared with the simulated one from CIF file and they are found to tally, which suggests the bulk purity of the crystalline form of **4** (supporting figure 4S).

Besides the above reactions, similar reaction of diphenic anhydride with copper(II) acetate in methanol was investigated in anticipation to prepare an ester containing Cu(II) precursor for studying its hydrolysis. An earlier work on the ring opening reaction of diphenic anhydride by cystine derivatives showed the formation of the corresponding acids, followed by their transformation to helical esters via the reaction with diazomethane.²³ In the present case, the reaction of diphenic anhydride with copper(II) acetate, followed by treatment with imidazole, resulted in the formation of an ester di-imidazole-di-(2-carbomethoxy-phenyl-2-benzoato)copper(II) complex, $[\text{Cu}(\text{cmp})_2(\text{im})_2]$ (where $\text{cmp} = 2\text{-carbomethoxy-phenyl-2-benzoate}$) (**5**). This compound has a distorted octahedral geometry around the copper(II) ion (Figure 8a), filled by two chelating $\eta^1:\eta^1$ -carboxylates in one plane and two mutually *trans* imidazole ligands. In the crystal structure the copper ion of the complex **5** lies on an inversion centre. The monocopper(II) units in **5** are interlinked via the $\text{N2-H2A}\cdots\text{O2}$ hydrogen bonds, forming a 1D H-bonded chain motif (Figure 8b) that can be described as a uninodal 2-connected net with the 2C1 topology (Figure 8c).^{17a}

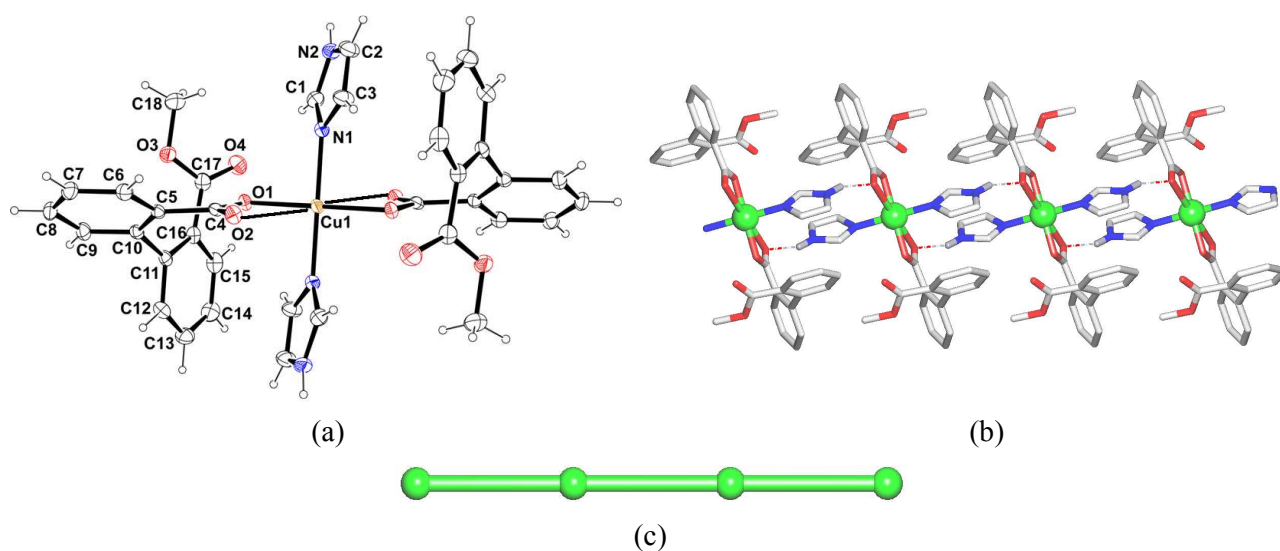


Figure 8: Structural fragments of the complex **5**. (a) Ellipsoid plot (50% probability). (b) H-bonding pattern showing the interlinkage of monocopper(II) units into a 1D H-bonded chain; H atoms apart from those of H-bonds are omitted for clarity; color codes: Cu green balls, O red, N blue, C gray, H dark gray. (c) Topological representation of the simplified uninodal 2-connected 1D net with the 2C1 topology; green balls are the centroids of 2-connected $[\text{Cu}(\text{cmp})_2(\text{im})_2]$ nodes.

Complex **5** is stable at ambient conditions and can be easily recrystallised from methanol solution. The comparison of structures of the complexes **5** and **1** shows that each compound has a six-coordinate copper(II) center with similar $\{\text{CuN}_2\text{O}_4\}$ environments but different geometries. For comparison, the $\angle\text{N1-Cu1-N1}$ bond angles are $164.63(11)$ and $180.00(6)^\circ$ in **1** and **5**, respectively, whereas the $\angle\text{O1-Cu1-}$

O1 bond angles are $177.97(10)^\circ$ (**1**) and $180.00(7)^\circ$ (**5**). Thus, there is relatively more space exposed on one side of copper ion in complex **1** which facilitates approaching of a water molecule and ease the hydrolysis reaction. In **1**, the ester groups are positioned on the same side across a plane, whereas in **5** they are on the opposite side. Hence, the hydrophobic part in the complex **1** adopts a pincer type of arrangement which would have helped its facile hydrolysis in crystalline state. In the case of complex **5**, the location of the two hydrophobic ester groups in opposite sides makes the approach of water less favorable from two directions providing an extra stability toward hydrolysis. Experimentally determined powder XRD of complex **5** along with simulated pattern is shown in supporting figure 6S, to confirm its bulk purity.

In conclusion, we have prepared and structurally characterized a series of copper(II)-imidazole compounds bearing different dicarboxylate monoester (**1**, **3**, **5**) or dicarboxylate (**2**, **4**) derivatives. In particular, two interesting examples of the solid state transformations (**1**→**2** and **3**→**4**) have been observed via fast hydrolysis of ester group in copper(II) precursors **1** and **3**. Topological analysis has revealed that in the case of the **1**→**2** transformation the overall 2D network topology changes from the 4-connected **sql** net to the 3-connected **hcb** net, while no topology modification has been observed during the **3**→**4** transformation, with both structures disclosing topologically equal H-bonded **sql** nets. This study also contributes to the understanding of the metal ion template transformations in solid state, providing a useful methodology to prepare new compounds that are different from those obtained during the conventional synthesis in solution.

Experimental:

Powder X-ray diffraction data were collected on a Bruker D2 diffractometer in Bragg-Brentano θ - θ geometry with Cu-K α radiation ($\lambda = 1.5418 \text{ \AA}$) on a glass surface of air-dried sample using a secondary curved graphite monochromator. Diffraction patterns were collected over a 2θ range of $5\text{--}50^\circ$ at a scan rate 1° min^{-1} . The powder patterns are compared with the theoretical indexed powder patterns generated from the crystallographic information files (CIF) by using MERCURY program. The indexing of the powder pattern is done by comparing the experimental pattern with the one generated from CIF.

Synthesis of $[\text{Cu}(\text{cmb})_2(\text{im})_2]$ (**1**): Phthalic anhydride (0.29 g, 2 mmol) was added to a methanolic solution (10 ml) of copper(II) acetate monohydrate (0.2 g, 1 mmol) and the reaction mixture was stirred for $\frac{1}{2}$ h. To this reaction mixture imidazole (0.15 g, 2 mmol) was added, followed by refluxing for 4 h. The reaction mixture was cooled to room temperature, filtered and kept undisturbed for crystallization. Dark-blue crystals of **1** were obtained in ca. 1 week. Yield, 62 %. For $\text{C}_{24}\text{H}_{22}\text{CuN}_4\text{O}_8$, % copper calcd. 11.38, found 11.42. IR (KBr, cm^{-1}): 3214 (br), 1730 (s), 1569 (m), 1390 (s), 1332 (m), 1288 (s), 1265 (s),

1123 (s), 1070 (s), 854 (m), 818 (s), 769 (s), 745 (s), 708 (m), 654 (s), 474 (m). Solid state UV-visible (nm): 275, 651.

Synthesis of $\{[\text{Cu}_2(\text{pht})_2(\text{im})_4 \cdot \text{H}_2\text{O}] \cdot \text{H}_2\text{O}\}_n$ (**2**): Dark-blue crystals of the complex **1** were moistened with a minimum amount of aqueous methanol and kept on a watch glass in open atmosphere. Their gradual change to light-blue colored crystals of **2** was completed in 2 days. Elemental analysis, % calcd. for $[\text{C}_{28}\text{H}_{28}\text{Cu}_2\text{N}_8\text{O}_{10}]_n$: C, 44.00; H, 3.67; N, 14.67; found: C, 45.1; H, 3.49; N, 15.03. IR (KBr, cm^{-1}): 3139 (w), 1616 (w), 1549 (br), 1443 (w), 1379 (s), 1329 (w), 1075 (s), 862 (w), 749 (s), 659 (s), 621 (m). Solid state UV-visible (nm): 298, 723.

Synthesis of $[\text{Cu}(\text{cmn})_2(\text{im})_4]$ (**3**): This compound was synthesized in a similar procedure that was used for **1**, except applying 1,8-naphthalic anhydride (0.4 g, 2 mmol) in DMF-methanol solvent (1:1, v/v) instead of phthalic anhydride in methanol. In this case, the 1:2:4 ratio of Cu, 1,8-naphthalic anhydride and imidazole was used. Blue crystals appeared after one week. Yield, 67 %. For $\text{C}_{38}\text{H}_{34}\text{CuN}_8\text{O}_8$, % of copper calcd. 7.99, found 8.10. IR (KBr, cm^{-1}): 3129 (br), 1740 (s), 1598 (w), 1577 (s), 1541 (s), 1442 (s), 1395 (s), 1303 (s), 1125 (s), 1074 (s), 1014 (s), 849 (m), 759 (m), 659 (s), 455 (m). Solid state UV-visible (nm): 280, 553.

Synthesis of $[\text{Cu}(\text{nap})(\text{im})(\text{DMF})(\text{H}_2\text{O})]_2$ (**4**). Blue crystals of **3** were moistened with a minimum amount of aqueous DMF and kept on a watch glass in open atmosphere. Their gradual change to green crystals of **4** was completed in 1-2 days. Elemental analysis, % calcd. for $\text{C}_{36}\text{H}_{38}\text{Cu}_2\text{N}_6\text{O}_{12}$: C, 49.44; H, 4.35; N, 10.99; found: C, 50.01; H, 4.58; N, 10.96. IR (KBr, cm^{-1}): 3141 (br), 1662 (w), 1623 (m), 1596 (m), 1409 (s), 1345 (s), 1223 (m), 1071 (s), 843 (w), 784 (s), 657 (s), 623 (s), 465 (m). Solid state UV-visible (nm): 297, 711.

Synthesis of $[\text{Cu}(\text{cmp})_2(\text{im})_2]$ (**5**): This compound was synthesized by reacting biphenic anhydride (0.45 g, 2 mmol) with copper(II) acetate monohydrate and imidazole in DMF-methanol solvent (1:1, v/v), in a procedure similar to that used for the synthesis of complex **3**. Blue colored crystals were formed after one week. Yield, 64 %. Elemental analysis, % calcd. for $\text{C}_{36}\text{H}_{30}\text{CuN}_4\text{O}_8$: C, 60.88; H, 4.26; N, 7.89; found: C, 60.53; H, 4.32; N, 7.96. IR (KBr, cm^{-1}): 3214 (br), 1730 (s), 1610 (w), 1567(m), 1391 (s), 1289 (s), 1263 (m), 1124(s), 1074(s), 818(s), 768(s), 703 (s), 654 (s), 474 (m). Solid state UV-visible (nm): 276, 574.

Structure determination: The single crystal X-ray diffraction data were collected at 296(2) K with Bruker Nonius SMART CCD diffractometer (for the compounds **1**, **2**, **3** and **5**) or Super Nova diffractometer (for the compound **4**), with $\text{MoK}\alpha$ radiation ($\lambda = 0.71073 \text{ \AA}$). For the data collected on the SuperNova diffractometer, data refinement and cell reductions were carried out by CrysAlisPro.²⁴ The structures were solved by direct methods using SHELXTL²⁵ and were refined on F^2 by the full-matrix least-square technique using the SHELXL-97 program package.²⁶ In all cases, non-hydrogen atoms were

treated anisotropically. The hydrogen atoms were freely allowed to ride on specific positions. Wherever possible, the hydrogen atoms were located on a difference Fourier map and refined. In other cases, the hydrogen atoms were geometrically fixed. The WR_2 and R factors of the complex **3** are high due to poor quality of single crystals tested and their decomposition. Crystallographic parameters are listed in Table 1.

Table 1: Crystallographic parameters of complexes **1-5**

Complex No	1	2	3	4	5
Formulae	$C_{24}H_{22}Cu N_4O_8$	$C_{28}H_{28}Cu_2N_8O_{10}$	$C_{38}H_{34} Cu N_8O_8$	$C_{36}H_{38}Cu_2N_6O_{12}$	$C_{36}H_{30} Cu N_4O_8$
Mol. wt.	558.00	763.66	794.28	873.80	710.18
Crystal system	Monoclinic	Monoclinic	Monoclinic	Monoclinic	Monoclinic
Space group	$C2/c$	$P2_1/n$	$P2_1/c$	$P2_1/n$	$P21/c$
$a/\text{Å}$	12.5530(6)	8.8941(3)	8.5178(13)	11.9671(8)	8.077(2)
$b/\text{Å}$	8.4912(6)	22.4052(8)	26.117(4)	13.7220(6)	12.926(3)
$c/\text{Å}$	24.4976(13)	16.1449(6)	9.9434(16)	12.2072(8)	17.252(4)
$\alpha/^\circ$	90.00	90.00	90.00	90.00	90.00
$\beta/^\circ$	100.436(3)	105.428(2)	125.233(10)	112.352(8)	114.682(10)
$\gamma/^\circ$	90.00	90.00	90.00	90.00	90.00
$V/\text{Å}^3$	2568.0(3)	3101.33(19)	1806.8(5)	1853.97(19)	1636.6(7)
Z	4	4	2	2	2
Density $g\cdot cm^{-3}$	1.443	1.631	1.453	1.565	1.441
Abs. Coeff. $/mm^{-1}$	0.905	1.442	0.670	1.220	0.727
F(000)	1148	1560	822	900	734
Total no. of reflections	2297	5534	3210	3349	2939
Reflections, $I > 2\sigma(I)$	2071	3654	2035	2768	2423
Max. $2\theta/^\circ$	50.50	50.50	50.50	50.50	50.48
Ranges (h, k, l)	-14 ≤ h ≤ 14 -10 ≤ k ≤ 4 -24 ≤ l ≤ 29	-10 ≤ h ≤ 10 -26 ≤ k ≤ 24 -19 ≤ l ≤ 19	-10 ≤ h ≤ 9 -31 ≤ k ≤ 31 -11 ≤ l ≤ 11	-14 ≤ h ≤ 14 -16 ≤ k ≤ 16 -14 ≤ l ≤ 14	-9 ≤ h ≤ 9 -15 ≤ k ≤ 15 -20 ≤ l ≤ 20
Complete to 2θ (%)	99.4	98.3	98.2	99.9	99.1
Data/Restraints/Parameters	2297 / 4 / 201	5534 / 4 / 449	3210 / 2 / 251	3349 / 2 / 264	2939 / 0 / 224
Goof (I^2)	1.097	1.077	1.196	1.013	1.059
R indices [$I > 2\sigma(I)$]	0.0304	0.0516	0.1598	0.0510	0.0311
R indices (all data)	0.0337	0.0981	0.1885	0.0624	0.0401
WR_2 [$I > 2\sigma(I)$]	0.0588	0.0779	0.3678	0.1369	0.0940
WR_2 (all data)	0.0600	0.0894	0.3781	0.1541	0.1014

Supporting information: Powder X-ray diffraction patterns of all the complexes are available. CIF files of the complexes are deposited to Cambridge Structural Database and they have the following CCDC numbers: 972841 (complex **1**), 972840 (coordination polymer **2**), 972843 (complex **3**), 972839 (metallacycle **4**), 972842 (complex **5**).

References:

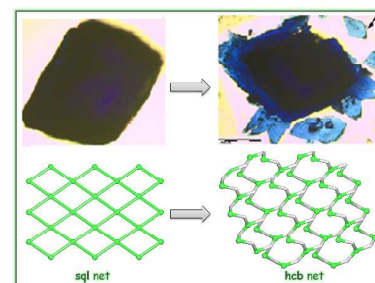
- (a) J. Chin, *Acc. Chem. Res.*, 1991, **24**, 145. (b) D. E. Wilcox, *Chem. Rev.*, 1996, **96**, 2435. (c) N. H. Williams, B. Takasaki, M. Wall, J. Chin, *Acc. Chem. Res.*, 1999, **32**, 485.
- (a) R. D. Wood, R. Nakon, R. J. Angelici, *Inorg. Chem.*, 1978, **17**, 1088. (b) R. Nakon, R. J. Angelici, *J. Am. Chem. Soc.*, 1973, **95**, 3170. (c) M. A. Mortellaro, T. J. Bleisch, B. F. Duerr, M. S. Kang, H. Huang, A. W. Czarnik, *J. Org. Chem.*, 1995, **60**, 7238. (d) B. F. Duerr, A. W. Czarnik, *Tetrahedron Lett.*, 1989, **30**, 6951. (e) J. Suh, S. Chung, S. H. Lee, *Bioorg. Chem.*, 1987, **15**, 383 (e) R. W. Hay, C. You-Quan,

- Polyhedron*, 1995, **14**, 869. (f) R. Ahmed, A. El-Sherif, M. M. Shoukry, *Inorg. Chim. Acta*, 2007, **360**, 2473. (g) P. Drabina, P. Funk, A. Ruzicka, J. Hanusek, M. Sedlak, *Transition Met. Chem.*, 2010, **35**, 363. (h) A. Pasini, L. Casella, *J. Inorg. Nuclear Chem.*, 1974, **36**, 2133. (i) A. Polyzos, A.B. Hughes, J. R. Christie, *Langmuir*, 2007, **23**, 1872. (j) Z. Zhang, Q. Fu, X. Li, X. Huang, J. Xu, J. Shen, J. Liu, *J. Biol. Inorg. Chem.*, 2009, **14**, 653.
3. (a) A. M. Baruah, A. Karmakar, J. B. Baruah, *Polyhedron*, 2007, **26**, 4518. (b) A. M. Baruah, A. Karmakar, J. B. Baruah, *Polyhedron*, 2007, **26**, 4479. (c) J. K. Nath, Y. Lan, A. K. Powell, J. B. Baruah, *Zeits. für Anorg. Allgem. Chem.*, 2013, **639**, 2250.
4. S. A. King, *J. Org. Chem.*, 1994, **59**, 2253.
5. J. K. Nath, J. B. Baruah, *Inorg. Chem. Commun.*, 2013, **30**, 128.
6. I. A. Yamskov, B. B. Berezin, L. A. Belchich, V. A. Davankov, *Die Makromolekulare Chemie*, 1979, **180**, 799.
7. M. A. R. Raycroft, L. Cimpean, A. A. Neverov, R.S. Brown, *Inorg. Chem.*, 2014, **53**, 2211.
8. (a) M. C. Brohmer, W. Bannwarth, *Eur. J. Org. Chem.*, 2008, 4412. (b) M. C. Brohmer, S. Mundinger, S. Brase, W. Bannwarth, *Angew. Chem. Int. Ed.*, 2011, **50**, 6125.
9. I. F. Barrera, C. I. Maxwell, A. A. Neverov, R. S. Brown, *J. Org. Chem.*, 2012, **77**, 4156.
10. M. A. R. Raycroft, C. I. Maxwell, R. A. A. Oldham, A. Saffouri Andrea, A. A. Neverov, R. S. Brown, *Inorg. Chem.*, 2012, **51**, 10325.
11. (a) J. R. Morrow, W. C. Trogler, *Inorg. Chem.*, 1988, **27**, 3387. (b) K.D. Deal, J. N. Burstyn, *Inorg. Chem.*, 1996, **35**, 2792. (c) F. M. Menger, L. H. Can, E. Johnson, D. H. Durst, *J. Am. Chem. Soc.*, 1987, **109**, 2800. (d) E. H. Serpersu, D. Shortle, A. S. Mildvan, *Biochemistry*, 1987, **26**, 1289.
12. (a) T. A. Shell, D. L. Mohler, *Curr. Org. Chem.*, 2007, **11**, 1525. (b) J. Sumaoka, Y. Yamamoto, Y. Kitamura, M. Komiyama, *Curr. Org. Chem.*, 2007, **11**, 463. (c) J. R. Morrow, O. Iranzo, *Curr. Opin. Chem. Biol.*, 2004, **8**, 192.
13. R. Reichenbach-Klinke, B. König, *J. Chem. Soc. Dalton Trans.*, 2002, 121.
14. (a) J. G. J. Weijnen, A. Koudijs, J. F. J. Engbersen, *J. Chem. Soc., Perkin Trans.*, 2, 1991, 1121. (b) C. A. Bunton, G. Savelli, *Adv. Phys. Org. Chem.*, 1986, **22**, 213. (c) J. H. Fendler, *Membrane Mimetic Chemistry*, Wiley, New York, 1982.
15. D. K. Wang, F. Rasoul, D. J. T. Hill, G. R. Hanson, C. J. Noble, A. K. Whittaker, *Soft Matter*, 2012, **8**, 435.
16. W. Tagaki, K. Ogino, *Top. Curr. Chem.*, 1985, **128**, 143.
17. (a) V. A. Blatov, *IUCr CompComm Newsletter*, 2006, **7**, 4. (b) V. A. Blatov, D. M. Proserpio, in *Modern methods of crystal structure prediction*. A. R. Oganov, Ed. Wiley, 2010, pp 1-28. (c) V. A. Blatov, M. O'Keeffe, D. M. Proserpio, *CrystEngComm*, 2010, **12**, 44. (d) E. V. Alexandrov, V. A. Blatov, A.V. Kochetkova, D. M. Proserpio, *CrystEngComm*, 2011, **13**, 3947. (e) M. O'Keeffe, O. M. Yaghi,

- Chem. Rev.*, 2012, **112**, 675. (f) M. O’Keeffe, M. A. Peskov, S. J. Ramsden, O. M. Yaghi, *Acc. Chem. Res.*, 2008, **30**, 1782.
18. (a) F. S. Delgado, J. Sanchiz, C. Ruiz-Perez, F. Lloret, M. Julve, *Inorg Chem.*, 2003, **42**, 5938. (b) A. Bondi, *J. Phys. Chem.*, 1964, **68**, 441.
19. S. G. Baca, M. T. Reetz, R. Goddard, I. G. Filippova, Y. A. Simonov, M. Gdaniec, N. Gerbeleu, *Polyhedron*, 2006, **25**, 1215.
20. J. -H. Li, J. -J. Nie, D. -J. Xu, *Acta. Crystallogr.*, 2008, **E64**, m948.
21. M. L. Cheney, G. J. McManus, J. A. Perman, Z. Wang, M. J. Zaworotko, *Cryst. Growth Des.*, 2007, **7**, 616.
22. M. C. Etter, G. M. Frankenbach, J. Bernstein, *Tetrahedron Lett.*, 1989, **30**, 3617.
23. I. L. Karle, P. Venkateshwarlu, R. Nagaraj, A.V. S. Sarma, D. Vijay, N. G. Sastry, S. Ranganathan, *Chemistry*, 2007, **13**, 4253.
24. CrysAlisPro, Oxford Diffraction Ltd., version 1,171. 33. 34d (release crysAlis 171.NET), 2009.
25. Sheldrick, G. M. *SHELXTL Reference Manual: Version 5.1*; Bruker AXS: Madison, WI, 1997.
26. Sheldrick, G. M. *SHELXL-97: Program for Crystal Structure Refinement*; University of Göttingen: Göttingen, Germany, 1997.

Graphical TOC:

Unusual solvent-mediated hydrolysis of dicarboxylate monoester ligands in copper(II) complexes toward simultaneous crystallization of new dicarboxylate derivatives



Unusual transformations of dicarboxylate monoester copper(II) compounds into crystalline dicarboxylate derivatives were observed in the solid state and investigated in detail by microscopy, IR and solid state UV-visible spectroscopy, X-ray crystallographic and topological analysis methods.

Jayanta Kumar Nath, Alexander M. Kirillov and Jubaraj B. Baruah